



U·P·O·J

¹Wei-Ju Tseng
¹Chantal de Bakker
¹Lin T
¹Wei T
¹Jia H
¹Levin LS
¹Qin L
^{*1}Liu XS

^{*1} McKay Orthopaedic Research Laboratory,
Department of Orthopaedic Surgery,
University of Pennsylvania,
Philadelphia, PA

Simultaneous Measurement of Changes in Bone Remodeling and Microvasculature in Response to Estrogen Deficiency-Induced Bone Loss and Intermittent PTH-Induced Bone Gain

Introduction

Bone is a dynamic, highly vascularized tissue that is involved in regulating calcium-phosphate metabolism and hematopoiesis. Osteogenesis and angiogenesis are closely coupled in bone remodeling process. Changes in bone remodeling are accompanied by changes in the microvascular network within bone marrow. Because of the drastic effects on bone remodeling, it is likely that both ovariectomy (OVX) and intermittent parathyroid hormone (iPTH) treatment will also affect bone vasculature. However, little is known about the impact of the relationships between bone remodeling and bone vasculature on OVX and iPTH treatment. Also, simultaneous visualization of the trabecular and vascular microstructures remains challenging. Therefore, it is of importance to understand the morphology of the bone vasculature. We hypothesized that the volume and number of blood vessels are associated with those of trabeculae. In this study, we used a well-described bone loss model by inducing estrogen deficiency in ovariectomized (OVX) rats and a bone gain model by administering intermittent parathyroid hormone (PTH) in intact rats.^{1,2} We developed a novel vascular network perfusion technique combining standard μ CT, image processing techniques and μ CT-based *in vivo* dynamic bone histomorphometry technique to allow for simultaneous visualization and quantification of the 3D trabecular and vascular microstructures, and longitudinal and simultaneous assessment of changes in bone remodeling in the rat tibiae. The overall goal was to develop a platform to investigate the changes in bone remodeling and microvasculature in response to estrogen deficiency-induced bone loss and iPTH-induced bone gain in rat tibiae.

METHODS

Study Design: 10 intact and 9 ovariectomized (OVX) female Sprague-Dawley rats (10-wk old) were purchased and housed at the animal facility (IACUC approved). The 9 OVX rats

developed osteopenia for 6 weeks. The 10 intact rats were divided into saline-treated (VEH) and PTH-treated groups (PTH 1-34, 60 μ g/kg/day, Bachem). Starting at 14-week old, both VEH and PTH groups received subcutaneous injections 5 days a week for 2 weeks.

Pre-perfusion scans: At age 15 and 16 weeks, 2 sequential scans of the proximal tibia were performed *in vivo* using the vivaCT 40 scanner (Scanco) for 3 groups of rats: OVX (n = 9), VEH (n = 5), and PTH (n = 5). A 4.4-mm region at week 15 and a 10-mm region at week 16, respectively, located distal to the proximal growth plate was acquired from each tibia at 10.5 μ m resolution.

Perfusion: Right after the week 16 scan, rats were perfused with Microfil[®] (MV122, Flow Tech), a radiopaque contrast agent, to form a vascular cast inside bone. Briefly, a heat pad was used to keep the animal's body temperature at 37°C. All perfusion solutions were prepared and maintained at 37°C in water bath except the Microfil[®] mixture. A catheter was inserted into the abdominal aorta, and an incision was made in the right atrium. Using a perfusion pump, heparin sodium (30 units/mL) followed by 100 mL of 0.9% saline and 50 mL 4% paraformaldehyde was infused at 4.4 mL/min through the rat. Next, using a syringe pump, 5 mL of freshly mixed Microfil[®] was infused into the aorta at 1 mL/min. Once the mixture reached the common iliac arteries, the flow rate was decreased to 0.3 mL/min. The Microfil[®] mixture was prepared by diluting a silicone rubber injection compound 4:1 with medium-viscosity diluent and mixing the result with 3% curing agent. The perfused animals were stored at 4 °C for 24 hours. Tibiae were harvested and fixed in 10% formalin.

Post-perfusion Scans: A 10-mm region located distal to the proximal growth plate was scanned at a 6 μ m resolution using the μ CT 35 scanner (Scanco). **Post-decalcification Scans:** The tibiae were then decalcified by 10% EDTA for three weeks. After the decalcification, the region distal to the proximal tibial growth plate, same as post-perfusion scans, were acquired at a 6 μ m resolution.

Correspondence:
*xiaoweil@mail.med.upenn.edu

Registration: A registration procedure was employed using a landmark-initialized, mutual-information-based registration kit (ITK, NLM). First, the pre-perfusion scans (containing bone structure only) were registered to the post-perfusion scans (containing bone structure and bone vasculature) to derive the first transformation matrix T_1 since bone structure was contained in both image sets. Next, the post-perfusion scans were registered to the post-decalcification scans (containing bone vasculature only) to derive the second transformation matrix T_2 since bone vasculature was contained in both image sets. Finally, transformation matrices T_1 and T_2 were combined to generate T_3 ($T_3 = T_2 \cdot T_1$), the transformation matrix which aligned the pre-perfusion scans to the post-decalcification scans which allowed the same region of interest to be analyzed in both scans.

Standard bone microstructure and blood vessel microstructure analyses: A volume of interest (VOI) in the secondary spongiosa of the pre-perfusion scans at 10.5 μ m resolution was segmented and evaluated for bone microstructural parameters including bone volume fraction (BV/TV), trabecular number (Tb.N), trabecular thickness (Tb.Th), and trabecular spacing (Tb.Sp). The registered VOI of the post-decalcification scans at 6 μ m resolution was segmented and evaluated for blood vessel microstructural parameters including vessel volume over marrow volume (Ves.V/Mar.V), vessel number (Ves.N), vessel thickness (Ves.Th), and vessel spacing (Ves.Sp).

μ CT-based *in vivo* dynamic bone histomorphometry: Bone resorption (BRR/BS) and formation (BFR/BS) were identified and measured based on the sequential *in vivo* μ CT scans.

Statistics: A one-way analysis of variance (ANOVA) with a Tukey Honestly Significance Difference (HSD) was performed to determine the between-group difference in bone and blood vessel microstructural measures and dynamic bone parameters with $p < 0.05$ indicating significance and $p \leq 0.1$ indicating trends.

Results

OVX vs. VEH: As expected, trabecular bone in the OVX group had 76% lower Tb.BV/TV ($p < 0.05$), 71% lower Tb.N ($p < 0.05$), 321% higher Tb.Sp ($p < 0.05$) compared to that of the VEH group. There was no measurable difference in Tb.Th (11%, $p < 0.1$). Vessels in the OVX group were 82% thicker than those in the VEH group ($p < 0.05$, Fig 2). Blood vessel in the OVX group had 43% higher Ves.V/Mar.V ($p < 0.05$), 81% higher Ves.N ($p < 0.05$), 30% lower Ves.Th ($p < 0.05$), and 48% lower Ves.Sp ($p < 0.05$) compared to that of the VEH group.

PTH vs. VEH: There was no significant difference in Tb.BV/TV, Tb.N or Tb.Sp between PTH and VEH groups, with a significant increase in Tb.Th in the PTH group (12%, $p < 0.05$). To confirm PTH's anabolic effect on bone, trabecular bone measurements after PTH treatment were also compared with those at the beginning of treatment measured by *in vivo* μ CT. Longitudinal comparisons confirmed that there was a 22% increase in Tb.BV/TV and 18% increase in Tb.Th ($p < 0.05$)

due to a 2-week PTH treatment. Moreover, compared to the VEH group, the PTH group had 29% lower Ves.Sp ($p < 0.05$). There was no significant difference in Ves.V/Mar.V, Ves.N and Ves.Th between PTH and VEH groups.

μ CT-based *in vivo* dynamic bone histomorphometry: BFR/BS was not significantly different between VEH-treated rats and OVX rats. Rats treated with PTH showed 266% ($p < 0.05$) greater BFR/BS than those treated with VEH (Fig. 1). Additionally, OVX rats had a 942% ($p < 0.05$) and 703% ($p < 0.05$) higher BRR/BS than rats treated with VEH and those treated with PTH, respectively (Fig. 1).

Discussion

In this study we developed an imaging framework to simultaneously visualize 3D trabecular microstructure and microvasculature inside the tibiae of both OVX rats and iPTH-treated rats. The resorption and formation map with vessels provides a platform for our future comparison between vessels and bone formation and resorption. Following a 6-week development of osteoporosis, OVX rats showed deteriorations in trabecular bone microstructure and a significant increase in vessel volume fraction and vessel number compared to the VEH rats. However, our vasculature results were inconsistent with Ding *et al's* and Peng *et al's* report.^{3,4} The discrepancy may be due to use of different animal models and different perfusion techniques. In case of iPTH treatment, we did not find improved angiogenesis after 2-week iPTH treatment compared to saline-treated rats, which was consistent with Prisby *et al's* report.⁵ Both OVX and iPTH treatment result in accelerated bone remodeling, but with opposite net balance towards resorption and formation, respectively. Our results showed that in estrogen deficiency-induced bone loss there may be a possible association between bone remodeling and angiogenesis while with iPTH-induced bone gain there may be not. More studies need to be done to test this hypothesis.

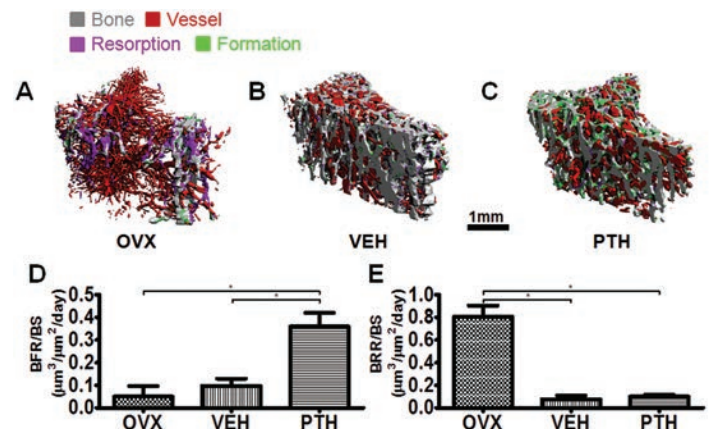


Figure 1. 3D trabecular bone and blood vessel images with bone resorption and formation labeled in purple and green, respectively (A) OVX, (B) VEH, and (C) PTH. Bone resorption and formation rate (D) BRR/BS (E) BFR/BS, Mean \pm SD, *: $p < 0.05$.

Significance

This study establishes a novel technique that simultaneously visualizes the 3D microstructures of bone and microvasculature using standard μ CT. Combined with measures of bone formation and resorption, this may help improve our understanding of the effects of OVX and iPTH on the bone-blood vessel function unit.

Acknowledgments

This study was partially supported by Penn Center for Musculoskeletal Disorders (NIH/NIAMS P30 AR050950). We'd like to thank A. Altman, PhD for her technical assistance.

References

1. **Kalu DN.** The ovariectomized rat model of postmenopausal bone loss. *Bone Miner*, 15:175-192, (1991).
2. **Qin L, Raggatt LJ, Partridge NC.** Parathyroid hormone: a double-edged sword for bone metabolism. *Trend in Endocrinol Metab*, 15(2):60-65 (2004).
3. **Ding WJ, Wei ZX, Liu JB.** Reduced local blood supply to the tibial metaphysis is associated with ovariectomy-induced osteoporosis in mice. *Connect Tissue Res*, 52(1):25-9 (2011).
4. **Peng J, et al.** Dimethylalylglycine prevents bone loss in ovariectomized C57BL/6J mice through enhanced angiogenesis and osteogenesis. *PLoS One*, 13;9(11):e112744 (2014).
5. **Prisby R, et al.** Intermittent PTH(1-84) is osteoanabolic but not osteoangiogenic and relocates bone marrow blood vessels closer to bone-forming sites. *J Bone Miner Res*. 26:2579-2582 (2011).